Palladium–thallium interactions in dinuclear complexes with structural components that place the two metal centers in close proximity

Alan L. Balch*, Brian J. Davis, Ella Y. Fung and Marilyn M. Olmstead
Department of Chemistry, University of California, Davis, CA 95616 (USA)

(Received January 27, 1993)

Abstract

Structural studies on two heterodinuclear complexes containing palladium and thallium are reported and compared to complexes containing platinum/thallium and iridium/thallium combinations. $[Tl(crown\text{-}P_2)Pd(CN)_2](PF_6)\cdot CHCl_3$ contains a planar $P_2Pd(CN)_2$ unit which is capped by a thallium(I) ion that is encapsulated within the azacrown portion of the crown-P_2 ligand ($Ph_2PCH_2N\{(CH_2)_2O(CH_2)_2O(CH_2)_2\}_2NCH_2PPh_2$). The Pd^{II}–Tl^{I} distance is 2.897(2) Å and a qualitative molecular orbital interpretation of the bonding interaction between the d^8 and s^2 ions is given. Orange $Pd(\mu\text{-}O_2CMe)_4Tl(O_2CMe)$ has a structure with four bridging acetates and one acetate ion that is chelated to the thallium. The Pd^{II}/Tl^{III} distance (2.702(1) Å) is shorter than that in the crown-P_2 bridged Pd^{II}–Tl^{I} complex, but comparison between the two structures suggests that there is no metal–metal bond in the acetate bridged structure.

Introduction

Examples of interactions between thallium as either Tl^{I} or Tl^{III} and transition metal ions are relatively rare. A brief review of these complexes containing transition metal/thallium bonds has been given [1]. The recent discovery of significant Tl^{I}–Pt^{II} bonding and intense photoluminescence in the simple molecular compound $\{Tl_2Pt(CN)_4\}$ [2–5] has aroused our interest in examining other complexes where transition metal/thallium bonding might occur. The structure of $\{Tl_2Pt(CN)_4\}$ differs from most salts that contain the planar $[Pt(CN)_4]^{2-}$ ion. Those salts usually crystallize as columnar materials with varying degrees of Pt–Pt bonding [6]. In $\{Tl_2Pt(CN_4\}$, however, the solid state structure consists of well-defined molecules with a planar $Pt(CN)_4$ core and two axial Pt–Tl bonds (Pt–Tl bond length, 3.140(1) Å) [2], but calculations do show that there is a very large ionic contribution to the Pt–Tl bond [3]. In order to stabilize the Pt–Tl bonded unit and to create a host environment that would facilitate the preparation of other related complexes which would contain both transition metal and main group metal components, the hybrid ligand, crown-P_2 (**1**) was designed and synthesized [7]. This ligand has been used to create a number of new complexes in which a d^8 transition metal (Pt^{II} or Ir^{I}) is placed near a non-transition metal ion as shown in Scheme 1 [1, 7, 8]. For main group ions with an s^2 electronic configuration (Tl^{I}, Sn^{II}, Pb^{II}) weak, but significant, metal–metal bond formation with both Pt^{II} and Ir^{I} has been detected through structural and spectroscopic studies. Since all of these cases involve metal ions from the third row of the transition series, where relativistic effects are believed to contribute significantly to bonding [9], we undertook an investigation into the preparation of complexes that would combine thallium with an analogous second row metal, Pd^{II}.

There was only one prior report on a complex that combined palladium and thallium. van Koten and coworkers reported that the reaction of palladium(II) acetate and thallium(III) acetate yielded yellow crystals of $Pd(\mu\text{-}O_2CMe)_4Tl(O_2CMe)$ (**5**), for which structures **A** and **B** (with **B** favored) were proposed [10]. This article reports the preparation of a new Pd^{II}/Tl^{I} complex that is formed with crown-P_2 as the bridging linker and also on the structure of $Pd(\mu\text{-}O_2CMe)_4Tl(O_2CMe)$.

Results

Preparation and characterization of $[Tl(crown\text{-}P_2)Pd(CN_2]^+$

The reaction of crown-P_2 with $(Ph_3P)_2Pd(CN)_2$ in toluene/methanol yields yellow $(crown\text{-}P_2)Pd(CN)_2$

*Author to whom correspondence should be addressed.

0020-1693/93/$6.00

© 1993 – Elsevier Sequoia All rights reserved

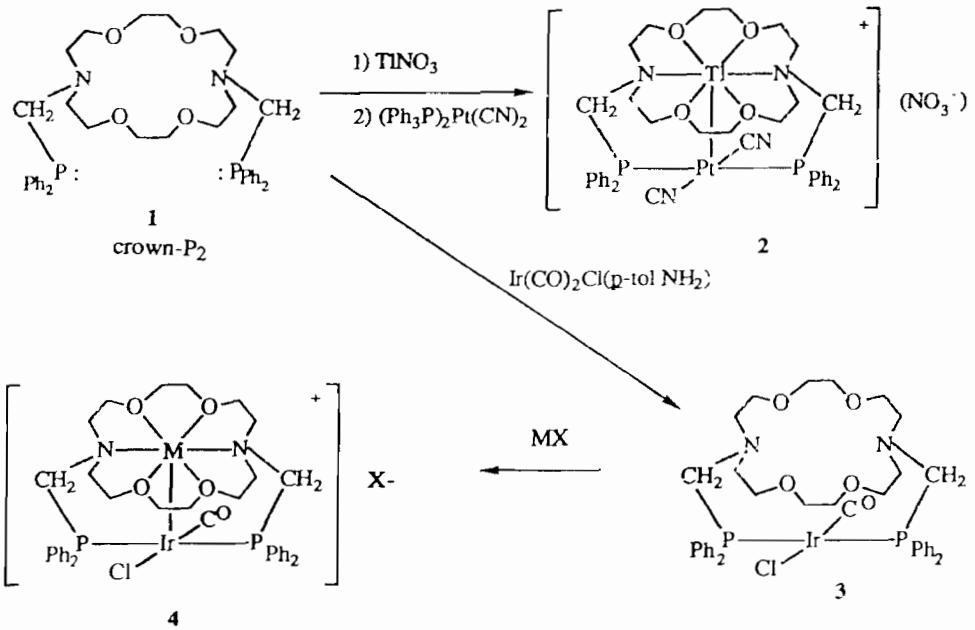

Scheme 1.

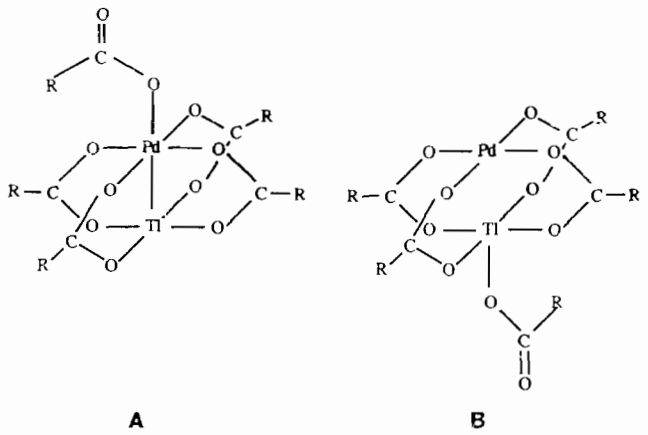

which was converted into $[Tl(crown\text{-}P_2)Pd(CN)_2](NO_3)$ (**6**) by treatment with thallium(I) nitrate in a dichloromethanol/methanol mixture. The IR spectrum of **6** shows a single cyanide stretching vibration at 2129 cm^{-1} (J(P, Tl) = 215 Hz). The $^{31}P\{^1H\}$ NMR spectrum of **6** in dichloromethane/methanol consists of a simple doublet at 17.0 ppm. The doublet splitting arises from coupling to thallium (^{205}Tl (70.5% natural abundance), ^{203}Tl (29.5%); both spin 1/2 with similar gyromagnetic ratios). Similar, long-range coupling has been observed for the platinum analog **2** (J(P, Tl) = 41 Hz) [7] and for the iridium complex **4** (M = Tl; J(P, Tl) = 84 Hz) [1].

Treatment of **6** with ammonium hexafluorophosphate converts it into $[Tl(crown\text{-}P_2)Pd(CN)_2]$ (PF_6) (**7**), which has been obtained as crystals that are suitable for X-ray crystallography. The asymmetric unit consists of one complex cation, one entirely normal hexafluorophosphate, and one molecule of chloroform. There are no unusually short contacts between these components, and none of these components has any crystallographically imposed symmetry. Atomic coordinates are presented in Table 1. Table 2 contains selected intratomic distances and angles.

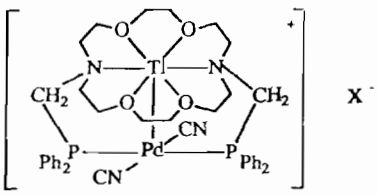

6 X = $(NO_3)^-$

7 X = $(PF_6)^-$

A drawing of the cation with the atomic numbering scheme is shown in Fig. 1. Figure 2 shows a stereoscopic view of the cation from a different perspective. The cation consists of a planar $P_2Pd(CN)_2$ portion with the thallium(I) center situated above the palladium and encapsulated by the crown ether portion. The Pd–Tl distance is 2.897(2) Å. For comparison, the Pt–Tl distances in the platinum analog **2** (which has two independent cations in the asymmetric unit) are 2.911(2) and 2.958(2) Å [7] and the Ir–Tl distance in the iridium complex **4** (M = Tl^I) is 2.875(1) Å [1].

While the disposition of ligands about the palladium center follows the rectilinear arrangement that is expected for planar d^8 complexes, the geometry about thallium is irregular. The Tl–O distances span the range 2.774(8) to 2.802(12) Å The Tl–N distances, 2.983(12) and 2.992(12) Å, are even longer. Consequently, the

TABLE 1 Atomic coordinates ($\times 10^4$) and equivalent isotropic displacement coefficients ($Å^2 \times 10^3$) for $[Tl(crown\text{-}P_2)Pd(CN)_2]\text{-}[PF_6]\ CHCl_3$

	x	y	z	U_{eq}[a]
Pt	−2094(1)	2345(1)	2205(1)	19(1)
Tl	517(1)	2481(1)	2573(1)	20(1)
Cl(1)	5059(5)	4271(4)	2132(3)	72(2)
Cl(2)	5012(6)	6261(4)	2584(4)	82(3)
Cl(3)	5473(6)	5079(4)	4009(3)	78(2)
F(1)	123(16)	7259(16)	2567(15)	188(12)
F(2)	1288(13)	8172(7)	1916(6)	80(5)
F(3)	1334(12)	8410(6)	3415(6)	72(5)
F(4)	2808(12)	7871(15)	2889(11)	141(9)
F(5)	1656(20)	6919(8)	3503(7)	139(10)
F(6)	1639(15)	6686(7)	2001(7)	101(7)
N(1)	−2045(12)	485(8)	884(9)	39(5)
N(2)	−1982(12)	4212(8)	3542(8)	37(5)
N(3)	153(10)	2940(7)	665(7)	22(4)
N(4)	124(10)	1983(7)	4377(7)	22(4)
O(1)	1186(8)	4317(6)	2285(5)	20(3)
O(2)	1406(8)	3769(6)	4094(6)	26(3)
O(3)	1205(8)	740(7)	3057(6)	29(3)
O(4)	1528(9)	1301(6)	1329(6)	25(3)
P(1)	−2283(3)	3038(3)	854(2)	21(1)
P(2)	−2297(3)	1621(3)	3480(2)	27(1)
P(3)	1465(4)	7539(3)	2706(3)	37(2)
C(1)	−2495(12)	4296(9)	892(8)	22(3)
C(2)	−3311(13)	4619(10)	206(9)	29(3)
C(3)	−3305(14)	5578(11)	248(10)	39(4)
C(4)	−2884(14)	6191(12)	942(10)	39(4)
C(5)	−2041(14)	5899(11)	1615(10)	36(4)
C(6)	−1840(13)	4939(10)	1570(9)	29(3)
C(7)	−3628(12)	2447(10)	134(9)	26(3)
C(8)	−4601(14)	2253(11)	575(10)	38(4)
C(9)	−5607(16)	1689(12)	99(11)	50(4)
C(10)	−5646(18)	1332(14)	−795(12)	59(5)
C(11)	−4717(16)	1569(13)	−1240(12)	53(5)
C(12)	−3711(15)	2093(11)	−754(10)	41(4)
C(13)	−2502(14)	319(11)	3358(10)	34(4)
C(14)	−3410(15)	−87(12)	3735(11)	47(4)
C(15)	−3506(18)	−1143(14)	3614(13)	62(5)
C(16)	−2789(19)	−1609(16)	3171(13)	69(6)
C(17)	−1888(17)	−1209(13)	2821(11)	52(5)
C(18)	−1758(15)	−243(12)	2899(11)	44(4)
C(19)	−3667(14)	2031(11)	3806(10)	36(4)
C(20)	−4686(15)	2023(11)	3115(11)	45(4)
C(21)	−5731(18)	2394(13)	3332(13)	58(5)
C(22)	−5752(19)	2757(14)	4210(13)	64(5)
C(23)	−4831(17)	2718(13)	4888(13)	56(5)
C(24)	−3750(16)	2350(12)	4706(11)	46(4)
C(25)	−1119(12)	2764(10)	175(9)	23(3)
C(26)	−1144(12)	2009(10)	4493(9)	25(3)
C(27)	554(13)	3956(10)	683(9)	29(3)
C(28)	1586(12)	4305(10)	1449(8)	23(3)
C(29)	2064(13)	4723(10)	3055(9)	30(3)
C(30)	1545(13)	4725(10)	3893(9)	30(3)
C(31)	862(13)	3700(10)	4849(9)	30(3)
C(32)	907(12)	2683(9)	5062(9)	26(3)
C(33)	556(14)	1029(10)	4493(10)	35(4)
C(34)	1621(13)	787(10)	4039(9)	28(3)
C(35)	2061(13)	356(11)	2555(9)	32(4)
C(36)	1567(14)	350(11)	1553(10)	37(4)
C(37)	915(14)	1311(10)	408(9)	34(4)
C(38)	962(13)	2340(10)	216(9)	30(3)
C(39)	−2094(13)	1160(11)	1378(9)	30(3)
C(40)	−2068(12)	3506(10)	3024(9)	23(3)
C(41)	5630(17)	5320(12)	2903(11)	53(5)

[a]Equivalent isotropic U defined as one third of the trace of the orthogonalized U_{ij} tensor.

TABLE 2. Selected interatomic distances (Å) and angles (°) for $[Tl(crown\text{-}P_2)Pd(CN)_2]^+$

Selected interatomic distances (Å)			
Pd–Tl	2.897(2)	Pd–P(1)	2.346(4)
Pd–P(2)	2.328(4)	Pd–C(39)	1.983(14)
Pd–C(40)	1 946(13)	Tl–N(3)	2.983(12)
Tl–N(4)	2.992(12)	Tl–O(1)	2.802(11)
Tl–O(2)	2.774(8)	Tl–O(3)	2.781(10)
Tl–O(4)	2.802(11)		
Angles (°)			
Tl–Pd–P(1)	95.1(1)	Tl–Pd–P(2)	95.5(1)
P(1)–Pd–P(2)	169.3(1)	Tl–Pd–C(39)	90.2(4)
Tl–Pd–C(40)	88.9(4)	P(1)–Pd–C(39)	83.5(4)
P(1)–Pd–C(40)	96.8(4)	P(2)–Pd–C(39)	95.8(5)
P(2)–Pd–C(40)	84.0(5)	C(39)–Pd–C(40)	179.1(7)
Tl–Pd–C(40)	88 9(4)	Pd–Tl–N(3)	82.2(4)
Pd–Tl–N(4)	81.7(4)	Pd–Tl–O(1)	105.1(4)
Pd–Tl–O(2)	111.1(4)	Pd–Tl–O(3)	105.8(4)
Pd–Tl–O(4)	113.4(4)	N(3)–Tl–N(4)	163.9(6)
N(3)–Tl–O(1)	61.8(6)	N(3)–Tl–O(2)	124.2(6)
N(3)–Tl–O(3)	123 3(6)	N(3)–Tl–O(4)	63.2(6)
N(4)–Tl–O(1)	123 1(6)	N(4)–Tl–O(2)	62 5(6)
N(4)–Tl–O(3)	61.8(6)	N(4)–Tl–O(4)	124 2(6)
O(1)–Tl–O(2)	62.5(6)	O(1)–Tl–O(3)	149.1(6)
O(1)–Tl–O(4)	105.0(6)	O(2)–Tl–O(3)	105.3(6)
O(2)–Tl–O(4)	135 6(6)	O(3)–Tl–O(4)	62 4(6)

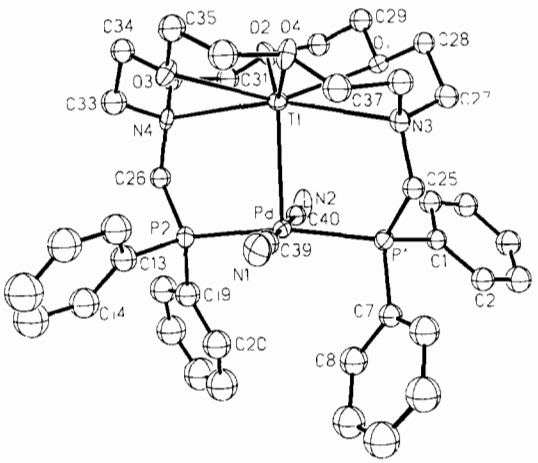

Fig. 1. A perspective view of the cation of $[Tl(crown\text{-}P_2)Pd(CN)_2](PF_6)\cdot CHCl_3$ showing 50% thermal contours for all atoms

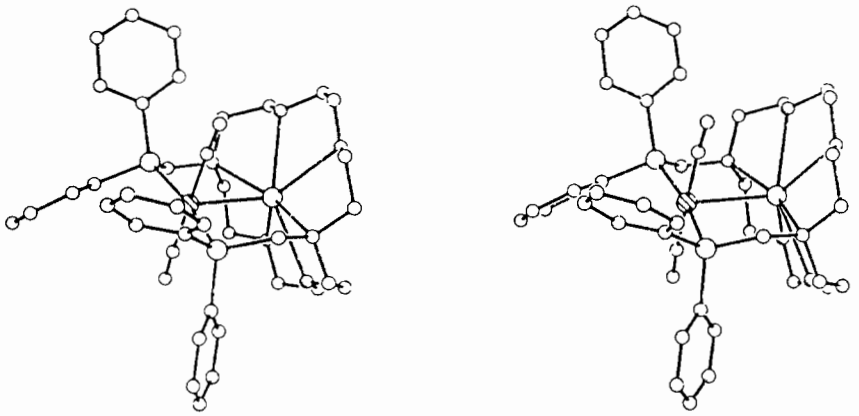

Fig 2. A stereoscopic view of the cation in $[Tl(crown\text{-}P_2)Pd(CN)_2](PF_6)\cdot CHCl_3$.

existence of a Tl–N bond is open to doubt. Despite the length of these Tl–N distances, it is important to note that these nitrogen atoms are oriented so that their lone pairs are directed inward toward the thallium rather than outward. Moreover, it is possible to compute the hypothetical location of the nitrogen lone pair by examining the location of the three adjacent carbon atoms. In **7** the angles between the hypothetical lone pair positions and the Tl–N lines are 4.7 and 4.8° for N(3) and N(4), respectively. This suggests that there are Tl–N bonds, probably with a high degree of ion-dipole character, in this complex. Overall the interaction of the Tl^{I} center with the azacrown portion of **7** is similar to that seen in the platinum and iridium analogs, **2** and **4** [1, 7].

Structural characterization of $Pd(\mu\text{-}O_2CMe)_4Tl(O_2CMe)$ (5)

The structure of the yellow–orange, acetate-bridged complex **5**, $Pd(\mu\text{-}O_2CMe)_4Tl(O_2CMe)$, has also been determined by X-ray crystallography. Atomic coordinates are given in Table 3. Table 4 contains a selection of interatomic distances and angles.

The asymmetric unit consists of one molecule of **5** with no crystallographically imposed symmetry. A drawing of a molecule of **5** is shown in Fig. 3. Figure 4 presents a stereoscopic drawing that shows the unit cell and the relative orientations of two molecules of **5**. There are no unusual contacts between these. As anticipated by van Koten and co-workers [10], the structure consists of a palladium and thallium center that is bridged by four acetate ions in typical fashion. The fifth acetate is coordinated to thallium as they expected, but this acetate is bidentate, not monodentate. The Pd–Tl distance is 2.702(1) (Å). Thus it is shorter than the Pt–Tl, Ir–Tl, or Pd–Tl distances seen in complexes that are bridged by crown-P_2.

The palladium center has the planar geometry that is common to four-coordinate, d^8 Pd(II) complexes. The Pd–O distances are all nearly equal and span the narrow range from 1.996(5) to 2.015(4) Å. The four, *cis* O–Pd–O bond angles also span a compact range, 88.7(2)–91.9(2)°, that is near the 90° ideal. The two *trans* O–Pd–O angles are 177.3(2) and 177.8(2)°. In contrast the coordination environment at thallium shows a larger range of angular distribution. The smallest O–Tl–O angle (56.9(2)°) involves the chelate ring of the terminal acetate. The other O–Tl–O angles range from 80.8(2) to 153.1(3)°. However the Tl–O distances cover a rather narrow range 2.249(4)–2.353(5) Å. These distances are much shorter than the Tl–O or Tl–N distances in $[Tl(crown\text{-}P_2)Pd(CN)_2]^+$.

TABLE 3. Atomic coordinates ($\times 10^4$) and equivalent isotropic displacement coefficients ($Å^2 \times 10^3$) for $Pd(\mu\text{-}O_2CCH_3)_4Tl(O_2CCH_3)$

	x	y	z	U_{eq}[a]
Tl	2009(1)	2670(1)	2613(1)	16(1)
Pd	4771(1)	658(1)	1451(1)	16(1)
O(1)	−60(8)	3354(6)	4148(4)	36(2)
O(2)	−396(7)	4846(6)	2696(4)	29(1)
O(3)	1466(7)	291(6)	3087(5)	33(2)
O(4)	3667(7)	−1149(5)	1957(4)	26(1)
O(5)	679(8)	2501(7)	1092(4)	40(2)
O(6)	3241(6)	1025(5)	191(3)	21(1)
O(7)	3797(7)	4257(6)	1836(4)	32(2)
O(8)	5998(6)	2415(5)	966(4)	24(1)
O(9)	6337(6)	213(6)	2679(3)	25(1)
O(10)	4386(7)	2042(6)	3707(4)	30(2)
C(1)	−1010(10)	4527(9)	3689(7)	33(2)
C(2)	−2801(12)	5604(10)	4123(8)	46(3)
C(3)	2287(9)	−983(8)	2688(5)	22(2)
C(4)	1679(11)	−2445(8)	3098(5)	30(2)
C(5)	1517(9)	1787(8)	278(5)	25(2)
C(6)	478(10)	1894(9)	−688(6)	32(2)
C(7)	5340(8)	3784(7)	1266(5)	19(2)
C(8)	6497(9)	4972(8)	925(5)	24(2)
C(9)	5852(8)	969(7)	3531(5)	18(2)
C(10)	7189(9)	530(8)	4383(5)	24(2)

[a]Equivalent isotropic U defined as one third of the trace of the orthogonalized U_{ij} tensor.

TABLE 4. Selected interatomic distances (Å) and angles (°) for $Pd(\mu\text{-}O_2CCH_3)_4Tl(O_2CCH_3)$

Selected interatomic distances (Å)			
Tl–Pd	2.702(1)	Tl–O(1)	2 353(5)
Tl–O(2)	2.249(4)	Tl–O(3)	2 254(5)
Tl–O(5)	2.285(6)	Tl–O(7)	2 257(6)
Tl–O(10)	2.281(5)	Pd–O(4)	1 996(5)
Pd–O(6)	2.015(4)	Pd–O(8)	2 005(5)
Pd–O(9)	1.997(5)		
Angles (°)			
Pd–Tl–O(1)	152 9(1)	Pd–Tl–O(2)	149 5(1)
O(1)–Tl–O(2)	56.9(2)	Pd–Tl–O(3)	76.5(1)
O(1)–Tl–O(3)	80.8(2)	O(2)–Tl–O(3)	120.1(2)
Pd–Tl–O(5)	76.1(1)	O(1)–Tl–O(5)	117.3(2)
O(2)–Tl–O(5)	79.5(2)	O(3)–Tl–O(5)	86.4(2)
Pd–Tl–O(7)	77.3(1)	O(1)–Tl–O(7)	122.4(2)
O(2)–Tl–O(7)	86.1(2)	O(3)–Tl–O(7)	153.1(2)
O(5)–Tl–O(7)	93.2(2)	Pd–Tl–O(10)	77.8(1)
O(1)–Tl–O(10)	86.4(2)	O(2)–Tl–O(10)	125.3(2)
O(3)–Tl–O(10)	86.8(2)	O(5)–Tl–O(10)	153.9(2)
O(7)–Tl–O(10)	81.8(2)	Tl–Pd–O(4)	91 1(1)
Tl–Pd–O(6)	91.9(1)	O(4)–Pd–O(6)	90 3(2)
Tl–Pd–O(8)	90.5(1)	O(4)–Pd–O(8)	177 3(2)
O(6)–Pd–O(8)	91.9(2)	Tl–Pd–O(9)	90.1(1)
O(4)–Pd–O(9)	88 7(2)	O(6)–Pd–O(9)	177 8(2)
O(8)–Pd–O(9)	89 1(2)		

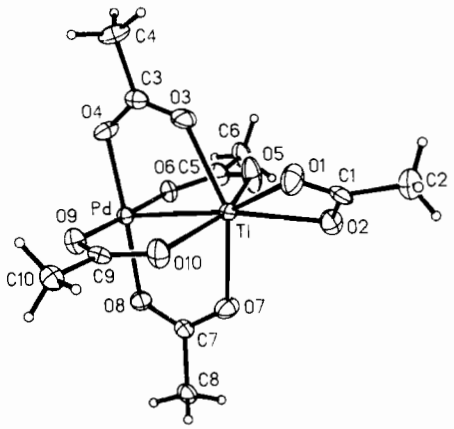

Fig. 3. A perspective view of $Pd(\mu\text{-}O_2CMe)_4Tl(O_2CMe)$ with 50% thermal contours for all atoms.

Discussion

A comparison of the two complexes, $[Tl(crown\text{-}P_2)Pd(CN)_4]^+$ and $Pd(O_2CMe)_4Tl(O_2CMe)$, is revealing. Although the acetate bridged complex **5** has the shorter Pd–Tl distance, we believe that there is evidence to suggest that **5** does not have a significant bond between these two metal centers. Such a finding would be in accord with the suggestions of van Koten and co-workers [10] and would correspond to a Pd^{II}/Tl^{III} formulation for this dinuclear species. The evidence for such a formulation comes from the following observations. Figure 3 shows that the thallium center in **5** is pulled away from the palladium and toward the bidentate acetate. This displacement is seen in the following comparison of angles. The four Tl–Pd–O angles span a range (90.1(1)–91.9(1)°) that is near 90° but the Pd–Tl–O angles are narrower (range 76.1(1)–77.8(1)°). Additionally, the Tl–O–C angles within the bridges span a range of angles (123.2(4)–126.6(5)°) that is wider than the corresponding Pd–O–C angles (range 120.5(4)–122.3(4)°). These angular distortions serve to allow for longer Pd–Tl distances than would be seen if the Pd–Tl–O angles were nearer to 90° and if the Tl–O–C angles were also contracted. The ionic radius for Tl^{III} is *c.* 0.47 to 0.61 Å less than that of Tl^{I} [11]. The shorter Tl–O distances (av. 2.280 Å) in the acetate bridged complex **5** relative to those (av. 2.780 Å) in the crown-P_2 complex **7** are fully in accord with this trend in ionic radii. This shortening suggests that it is appropriate to view **5** as a Pd^{II}/Tl^{III} complex while **7** involves Pd^{II} and Tl^{I}. Complex **7** might alternatively have ended up as a Pd^{III}/Tl^{II} complex if the thallium reagent had oxidized the palladium. In that case transfer of an acetate ligand from thallium to palladium to give the previously considered structure **B** would have been expected. In this context, it is important to point out that treatment of $Ir(CO)Cl(PPh_3)_2$ with thallium(III) acetate in the presence of silver(I) acetate yields **8** in which an analogous oxidative transformation to form an Ir^{II}/Tl^{II} complex has occurred [1, 12]. In that case the Ir–Tl bond distance (2.611(1) Å) is shorter than the Pd–Tl distance in **5**; although **8** has a less constraining bridging arrangement but sterically more encumbering ligation.

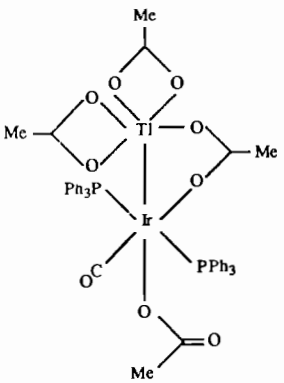

8

For the crown-P_2 bridged cation **7**, the Pd–Tl interaction appears to be comparable to the Pt–Tl and Ir–Tl interactions in **2** and **4**. The bond distances are comparable, and in fact the Pd–Tl distance is actually shorter than the Pt–Tl distance. Thus, the differences

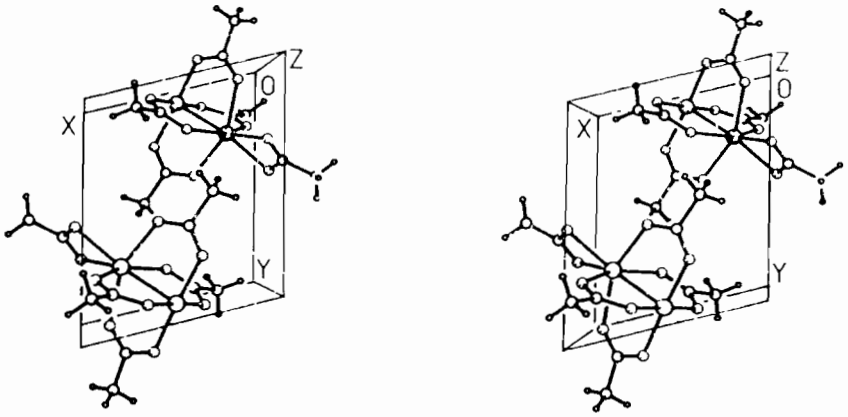

Fig. 4. A stereoscopic view of the relative orientation of two molecules of $Pd(\mu\text{-}O_2CMe)_4Tl(O_2CMe)$ in the solid state.

in relativistic effects on the second and third row metal centers (Pd versus Pt) do not manifest themselves in structural variations. Note also that the long range Tl–P coupling in these crown-P_2 species is largest for the palladium complex. If this coupling is principally transfered through the Tl–M–P bonds, this also suggests that Pd–Tl bonding is significant in **7**.

We view the Pd^{II}–Tl^{I} bonding in **7** to result from interaction between the filled d_{z^2} orbital on palladium with the filled s^2 orbital on thallium as shown in Fig. 5. These will combine to form the σ orbitals, a(1) and a*(1), both of which will be occupied. However similar overlap of the empty p_z orbitals on palladium and thallium will produce the empty σ molecular orbitals, a(2) and a*(2). Mixing of the a(1) and a(2) sets is allowed on the basis of symmetry. Such mixing will stabilize both the a(1) and a*(1) orbital so that the palladium–thallium interaction is attractive. The picture that emerges from these considerations is consistent with previous qualitative and quantitative analysis on Pt–Tl bonding [2, 3].

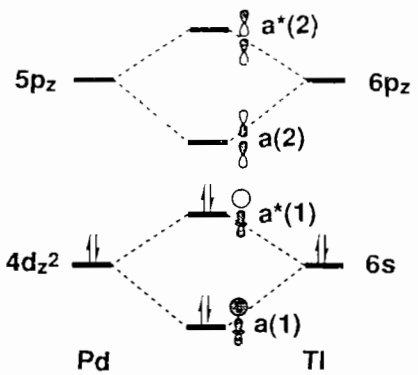

Fig. 5. A qualitative molecular orbital diagram that focuses on the Pd–Tl bonding in $[Tl(\text{crown-}P_2)Pd(CN)_2]^+$. The z axis is colinear with the Pd–Tl bond.

Experimental

Preparation of compounds

Samples of crown-P_2 [7], $(Ph_3P)_2Pd(CN)_2$ [13] and $Pd(\mu\text{-}O_2CCH_3)_4Tl(O_2CCH_3)$ [10] were obtained by the routes described earlier.

[Tl(crown-P_2)Pd(CN)$_2$](PF$_6$)

A solution of 108.0 mg (0.1581 mmol) of *trans*-$(Ph_3P)_2Pd(CN)_2$ in a mixture of 15 ml of toluene and 10 ml of methanol was added to a solution of 103.6 mg (0.1573 mmol) of crown-P_2 in 10 ml of toluene. This solution was stirred for 4 h. The volume of the resulting orange solution was reduced to 10 ml through vacuum evaporation. Diethyl ether was added to this solution until the mixture became cloudy. This sample was then stored at −20 °C for 12 h. The pale orange, crystalline product was harvested by filtration, washed with diethyl ether, and vacuum dried to yield 111.6 mg (90%) of (crown-P_2)$Pd(CN)_2$. IR(hydrocarbon mull): ν(CN), 2128 cm^{-1}; $^{31}P\{^1H\}$ NMR: δ, 11.9 ppm. A solution of 10.1 mg (0.0379 mmol) of thallium(I) nitrate in a minimum volume of 1:1 vol./vol. methanol/chloroform was added to a solution of 22.5 mg (0.0275 mmol) of (crown-P_2)$Pd(CN)_2$ in 5 ml of chloroform. This yellow solution was stirred for 12 h. After the dropwise addition of diethyl ether a pale yellow, crystalline precipitate of $[Tl(\text{crown-}P_2)Pd(CN)_2](NO_3)$ was obtained; yield 16.5 mg (51%). IR (hydrocarbon mull): ν(CN), 2129 cm^{-1}; $^{31}P\{^1H\}$ NMR: δ, 17.0 ppm, J(Tl, Pd) = 215 Hz. This was converted essentially quantitatively into $[Tl(\text{crown-}P_2)Pd(CN)_2](PF_6)$ by the addition of a solution of ammonium hexafluorophosphate in methanol to the solution of the complex in chloroform.

X-ray data collection

[Tl(crown-P_2)Pd(CN)$_2$](PF$_6$)·CHCl$_3$

Pale yellow blocks were obtained by slow diffusion of diethyl ether into a solution of the complex in a mixture of chloroform and methanol.

$Pd(\mu\text{-}O_2CMe)_4Tl(O_2CMe)$

Suitable crystals were grown by suspending the complex in hexane and adding sufficient dichloromethane to completely dissolve the solid. Slow evaporation of the solvent produced orange needles.

The crystals were coated with a light hydrocarbon oil and a selected crystal was placed in the 130 K dinitrogen stream of a Syntex $P2_1$ diffractometer that was equipped with a LT-1 low-temperature apparatus. The two check reflections showed only random fluctuation (<2%) in intensity during the data collection. The data were corrected for Lorentz and polarization effects. Crystal data are given in Table 5.

Solution and refinement of structures

$[Tl(crown\text{-}P_2)Pd(CN)_2](PF_6)\cdot CHCl_3$

The calculations were performed on a MicroVAX 3200 computing system using the Siemens SHELXTL PLUS software package. The structure was solved by direct methods. Anisotropic thermal parameters were assigned to the palladium, thallium, chlorine, fluorine, nitrogen, oxygen and phosphorus atoms. Isotropic thermal parameters were used for all other atoms. All hydrogen atoms were fixed at calculated positions by using a riding model in which the C–H vector was fixed at 0.96 Å, and the isotropic thermal parameter for each hydrogen atom was fixed at a value of 0.04 during the refinement. Scattering factors and corrections for anomalous dispersions were taken from a standard source [14]. The final stages of refinement included an absorption correction. The method obtains an empirical absorption tensor from an expression that relates F_o and F_c [15]. The largest feature in the final difference Fourier map (2.03 e Å^3) was located 1.022 Å from the thallium atom.

$Pd(\mu\text{-}O_2CMe)_4Tl(O_2CMe)$

The calculations were performed as described above and the structure was solved using direct methods. Anisotropic thermal parameters were assigned to palladium, thallium, oxygen and carbon. Hydrogen atoms were treated in the fashion noted above. An absorption correction was applied as described previously [15].

Supplementary material

Listings of thermal parameters, hydrogen atom coordinates, bond distances and angles, and observed and

TABLE 5. Crystal data and data collection parameters for compounds

	7	5
Formula	$C_{41}H_{49}Cl_3F_6N_4O_4P_3PdTl$	$C_{10}H_{15}O_{10}PdTl$
Formula weight	1285.9	606.0
Color and habit	yellow blocks	orange needles
Crystal system	triclinic	triclinic
Space group	$P\bar{1}$ (No. 2)	$P\bar{1}$ (No. 2)
a (Å)	11 296(7)	7.324(2)
b (Å)	14.316(7)	8 772(2)
c (Å)	15.061(8)	12.721(4)
α (°)	96 74(4)	86 34(2)
β (°)	100.26(4)	83.93(2)
γ (°)	92.35(4)	75.47(2)
V (Å^3)	2375(2)	768 0(4)
T (K)	130	130
Z	2	2
Crystal dimensions (mm)	0 10×0.25×0 65	0.13×0.18×0 43
D_{calc} (g cm^{-3})	1.80	2 56
Radiation (Å)	Mo Kα (λ=0 71069 Å)	Mo Kα (λ=0.71069 Å)
μ(Mo Kα) (cm^{-1})	41.32	197.7
Range transmission factors	0.30–0.69	0.14–0.31
Diffractometer	Syntex $P2_1$	Syntex $P2_1$
Scan range (°)	0 0–45.0	0.0–55.0
Scan speed (° min^{-1})	15	12
Octants collected	h, $\pm k$, $\pm l$	$\pm h$, $\pm k$, l
No. data collected	6226	3644
No. unique data	6226	3631
No. data refined	5069 ($F>4.0\sigma(F)$)	3440 ($F>4$ 0σF)
No. parameters refined	363	199
R[a]	0 063	0.036
R_w[b]	0.080 ($w^{-1}=\sigma^2(F)+0$ 0018F^2)	0 041 ($w^{-1}=\sigma^2(F)+0.0062F^2$)

[a]$R=\Sigma\|\|F_o\|-\|F_c\|\|/\Sigma|F_o|$. [b]$R_w=\Sigma\|\|F_o\|-\|F_c\|\|w^{1/2}/\Sigma|F_o|w^{1/2}$

calculated structure factors are available form the authors on request.

Acknowledgements

We thank the National Science Foundation (CHE 9022909) for support and Johnson Matthey Inc. for a loan of palladium(II) chloride.

References

1 A.L Balch, F. Neve and M.M Olmstead, *J Am. Chem Soc., 113* (1991) 2995
2 J.K. Nagle, A L Balch and M.M. Olmstead, *J Am Chem Soc., 110* (1988) 319.
3 T. Ziegler, J.K. Nagle, J G. Snijders and E.J. Baerends, *J Am. Chem Soc, 111* (1989) 5631.
4 J.K. Nagle, J.H. Lacasce, P J Dolan, M.R. Corson, Z Assefa and H H. Patterson, *Mol Cryst. Liq Cryst, 181* (1990) 359
5 B. Weissbart, A.L. Balch and D S Tinti, *Inorg Chem, 32* (1993) 2096.
6 G. Gliemann and M. Yersin, *Struct Bonding (Berlin), 62* (1985) 87.
7 A.L. Balch and S.P Rowley, *J Am Chem Soc, 112* (1990) 6139.
8 A.L Balch, F. Neve and M M. Olmstead, *Inorg Chem, 30* (1991) 3395
9 P. Pykko, *Chem Rev, 88* (1988) 563.
10 A.F M.J. van der Ploeg, G. van Koten and K. Vrieze, *Inorg. Chim. Acta, 39* (1980) 253.
11 R.D. Shannon, *Acta Crystallogr, Sect A, 32* (1976) 751.
12 P.I. van Vliet and K. Vrieze, *J Organomet Chem, 139* (1977) 337.
13 B.B. Chastain, E.A. Rick, R L. Pruett and H.B. Gray, *J Am Chem Soc, 90* (1968) 3994
14 *International Tables of X-ray Crystallography*, Vol. 4, Kynoch, Birmingham, UK, 1974.
15 B. Moezzi, *Ph D Thesis*, University of California, Davis, 1987